Eur. Phys. J. C (2025) 85:308
https://doi.org/10.1140/epjc/s10052-025-14015-1

THE EUROPEAN PHYSICAL JOURNAL C

Regular Article - Theoretical Physics

Study of mass accretion of fluids flow near the horizon of charged acoustic black hole

Puja Mukherjee[1,a], **Ujjal Debnath**[1,b], **Pameli Saha**[2,c]

[1] Department of Mathematics, Indian Institute of Engineering Science and Technology, Shibpur, Howrah 711 103, India
[2] Department of Mathematics, Amity University, Maharashtra 410206, India

Received: 30 January 2025 / Accepted: 25 February 2025

Abstract In the astrophysical universe, the falling matter accretion around the black hole is becoming an engrossing chapter. Our present manuscript reveals the matter accretion onto the acoustic-charged black hole in the background of Gross–Pitaevskii theory. This type of black hole is popular to several researchers. Following Hamiltonian dynamics, we go through the accretion process to face the cosmological mechanism. Depending on the tuning parameter ξ of this black hole, we formulate sonic points to have a physical analysis of the speed of sound at sonic points. Undergoing the isothermal test fluids, we generate field equations at sonic points for our proposed model. Then we observe the accretion flow of the distinctive fluids around the acoustic-charged black hole with the variation of the tuning parameter. The most fascinating part of this work is to look for an analysis of the rate of flow of mass accretion of the different kinds of fluid onto our proposed black hole at sonic points with a graphical analysis. By investigating the accretion rate of these fluids, we seek stable and reliable results to check the compactness with the observational data.

1 Introduction

The ever-evolving universe is currently in its accelerated phase of expansion [1–8] leaving us spell-bound and curious. There are many logical explanations for this expansion, and cosmologists are eager to discover its effects on different entities. Black holes are, in general, one of the most mysterious things that ever existed in the universe. Several studies were conducted on them, as they are a natural laboratory for verifying Einstein's general theory of relativity and a perfect candidate for observing how it interacts with the surrounding matter. Among them, charged black holes are one of the most prominent types. Naturally, it attracted the attention of researchers, leading to many remarkable works on them [9–14].

Analogous black holes contributed in an exceptional manner to establishing the theoretical results related to astrophysical phenomena in an experimental way. As a result, first, the concept of an acoustic black hole came into light [15]. Following this, several other types of research were conducted to investigate other related astrophysical scenarios [16–25]. Impressed by its features, researchers started to observe other aspects of acoustic black holes in detail [26–29]. Definition of an acoustic black hole from the thermodynamic perspective [30], the geometry of higher-dimensional acoustic black holes in curved spacetime [31], determination of Hawking temperature and showing the departure from thermality for an analogous acoustic black hole considering one-dimensional Bose–Einstein condensate [32], detail analogy of an acoustic black hole [33] etc. were explored. Researchers also started investigating different theories that can present us with different versions of acoustic black holes [34–39].

Acoustic black holes in curved spacetime are more of a reliable concept as the structure of the universe is much more complex than our thinking, and black holes are an integral part of the universe, so they possibly can be in the bath of cosmological superfluid or microwave, possessing a more complex and richer near-horizon structure. This concept is very significant from the perspective of astrophysical black holes, as an acoustic horizon can clearly affect the nature of the near-horizon area. Thus, acoustic black holes in curved spacetime became a popular concept among researchers. Relativistic Gross–Pitaevskii theory is one of the famous theories for observing acoustic black holes in general curved spacetime

[a] e-mail: pmukherjee967@gmail.com
[b] e-mail: ujjaldebnath@gmail.com
[c] e-mail: pameli.saha15@gmail.com (corresponding author)

Published online: 17 March 2025

[39]. Also, research on particle motion around Schwarzschild acoustic black holes was conducted in [40]. Studies regarding quasi-bound states, and analogous Hawking radiation for Schwarzschild acoustic black hole spacetime were given in [41]. Further, in [42], some important aspects like the shadow and near-horizon properties of acoustic Schwarzschild black holes were observed. Moreover, the near-horizon properties and shadow of an acoustic-charged black hole were analyzed in [43]. Recently, a detailed study of the thermodynamics of acoustic-charged black holes as a heat engine was discussed in [44].

Accretion is a very significant phenomenon in black hole astrophysics, as it can constrain astronomical observations and increase the mass of the target object together with the increase in the angular momentum of the accreting object. In fact, accretion is the basic concept behind the rise of celestial objects like black holes, stars, plants, etc. The classic work of accretion in Newtonian gravity was accomplished in [45]. The other researchers then follow the same path to observe different relativistic accretion models [46–49]. A generalization of Bondi's accretion model [45] was proposed in [50]. Similarly, general relativistic and symmetric fluid accretion on a black hole [51], describing the backreaction effects on the black hole by spherically symmetric polytropic perfect fluids [52] was achieved.

Several remarkable works on black hole mass accretion phenomena, such as investigating the behavior of phantom energy near stringy magnetically charged black holes [10], effects of the phantom-like fluid onto the Schwarzschild black hole [53], applying the relativistic hydrodynamics phenomena to inspect the dark energy accretion onto the Schwarzschild black hole [54], accretion of two special types of Chaplygin gases called modified Chaplygin–Jacobi gas and modified Chaplygin–Abel gas onto a 4-dimensional Schwarzschild black hole [55], matter accretion process of a charged black hole in metric affine gravity [56], investigation on primordial black holes in brane cosmology in the basis of matter accretion [57], mass accretion in Einstein–Aether gravity with the help of parameter constraining [58] and accretion through Hamiltonian approach due to some well-known fluids [59], matter accretion via Hamiltonian approach onto brane-world black hole [60], effects of various types of Chaplygin gas accretion onto the mass of a Kehagias–Sfetsos black hole in Horava–Lifshitz gravity [61], matter accretion scenarios in Einstein–power–Maxwell black hole [62] and mass accretion process in conformal gravity black hole [63], mass accretion on generalized Rastall gravity theory [64], mass accretion of modified Hayward black hole [65] and matter accretion onto a charged dilaton black hole [66] were analyzed. Furthermore, some other famous works on mass accretion given in [67–73] had contributed some great results in the study of astrophysical black holes. All of these are pieces of evidence for the importance of accretion phenomena in black hole-related studies as well as in today's cosmological research.

Impressed with all of these exceptional works, in our present paper, we discuss the matter accretion process of a charged acoustic black hole from the reference [43]. This work is highly influenced by the Hamiltonian approach of the accretion process [59,63,66,74]. Following the matter accretion processes onto the charged dilaton black hole [66] depending on the dilaton parameter and the conformal gravity black hole [63], we investigate the matter accretion flow around the acoustic charged black hole to obtain the analysis of supersonic and subsonic accretion flow near the horizon and far away horizon of the black hole depending on the tuning parameter. We categorize the work as follows: in Sect. 2, we discuss the background concept and basic equations for the charged acoustic black hole. In Sect. 3, we obtain the sonic points and analyze the concept of isothermal test fluids. Section 4 is devoted to the analysis of the charged acoustic black hole for different fluids. Then, in Sect. 5, we discuss the results one-by-one. In Sect. 6, the matter accretion process of the black hole is investigated, and at last, in Sect. 7, all the findings of our work are explained in detail, marking the conclusion of this work.

2 Accretion onto charged acoustic black hole

In this section, let us explore the acoustic black hole in the background of general curved spacetime, which has been started by the action on account of the Gross–Pitaevskii (GP) theory considering the fact that in the probe limit, the matter field has no backreaction with the corresponding spacetime [39,75–77] given as follows:

$$S = \int d^4x\sqrt{-g}\left(|\partial_\mu\phi|^2 + m^2|\phi|^2 - \frac{b}{2}|\phi|^4\right), \tag{1}$$

where b is a constant, ϕ is the complex scalar field and m is the GP theory parameter depending on temperature [39].

We are going to discuss the accretion process of an acoustic-charged black hole. The main concept of an acoustic black hole in the general curved spacetime originates from the relativistic Gross–Pitaevskii theory [39]. Considering the static spacetime background in the case of the Reissner–Nordstrom black hole, we have the following form of the metric as [43]:

$$ds^2 = \sqrt{3}c_s^2\left[-\mathcal{F}(r)dt^2 + \frac{dr^2}{\mathcal{F}(r)} + r^2(d\theta^2 + sin^2\theta d\phi^2)\right], \tag{2}$$

with

$$\mathcal{F}(r) = \left(1 - \frac{2M}{r} + \frac{Q^2}{r^2}\right)\left[1 - \xi\left(\frac{2M}{r} - \frac{Q^2}{r^2}\right)\left(1 - \frac{2M}{r} + \frac{Q^2}{r^2}\right)\right]. \tag{3}$$

where M and Q denotes the black hole mass and charge in a respective manner satisfying the relation $M \geq Q$ and equality holds for the extremal Reissner–Nordstrom black hole case. Here, the radial component of velocity is given as $v_r \equiv \sqrt{\left(\frac{2M}{r} - \frac{Q^2}{r^2}\right)\xi}$, ξ being the tuning parameter that needs to satisfy condition $\xi \geq 1$ in order of the free movement of the relativistic fluid outside the black hole background. This property follows from the consideration given in [43]. Also, following [39], we can rescale the normalized condition in such a way that when $\xi \to 0$, the metric Eq. (2) reduces to the Reissner–Nordstrom black hole and as $\xi \to +\infty$, the escape velocity of the black hole becomes infinity, implying that the event horizon of the black hole will also become infinity. Again, when $Q \to 0$, this metric reduces to the Schwrazschild acoustic black hole [39,42]. For our convenience, we have considered $\sqrt{3}c_s^2 = 1$ [43]. The horizon structures of our charged acoustic black hole have been portrayed physically through Fig. 1. We observe the physical behavior of the horizon structures with the values of $\zeta = 0, 0.5, 1, 1.5$ for our BH solution.

Now, let us analyze the accretion process of the black hole; here, we have a fluid rest frame; thus, we can define the proper baryon number density as well as the particle flux current density. Let n be the baryon number density in the fluid rest frame, then we have the following equations,

$$u^\mu = \frac{dx^\mu}{d\tau}, \tag{4}$$

$$J^\mu = nu^\mu, \tag{5}$$

The mass–energy conservation is given by [78]:

$$\nabla_\mu J^\mu = \nabla_\mu (nu^\mu) = 0. \tag{6}$$

where ∇_μ is the covariant derivative. The energy–momentum tensor for perfect fluid is given as:

$$\Theta^{\mu\nu} = (\epsilon + p)u^\mu u^\nu + pg^{\mu\nu}, \tag{7}$$

where ϵ is the energy density and p is the pressure. As the fluid is spherically steady and satisfies the normalization condition

$$u^\mu u_\nu = -1, \tag{8}$$

which gives,

$$u^t = \frac{\sqrt{\mathcal{F}(r) + u^2}}{\mathcal{F}(r)}, \tag{9}$$

and

$$u_t = -\sqrt{\mathcal{F}(r) + u^2}. \tag{10}$$

In the equatorial plane ($\theta = \pi/2$), Eq. (6) reduces to the following form:

$$\nabla_\mu (nu^\mu) = \frac{1}{\sqrt{-g}}\partial(\sqrt{-g}nu^\mu) = \frac{1}{r^2}\partial_r(r^2 nu) = 0, \tag{11}$$

By integration,

$$r^2 nu = C_1, \tag{12}$$

where C_1 is constant. As the velocity of the fluid for the case of accretion is negative, C_1 is also negative.

The thermodynamics of fluid are described by the following equations,

$$dp = n(dh - Tds), \quad and \quad d\epsilon = hdn + nTds. \tag{13}$$

where T is the temperature, s is the specific entropy. Let us define the enthalpy as follows:

$$h = \frac{\epsilon + p}{n}. \tag{14}$$

Now, the conservation of energy-momentum tensor for perfect fluid can be written as:

$$nu^\mu \nabla_\mu (hu^\nu) + g^{\mu\nu}\partial_\mu p = 0. \tag{15}$$

We consider isentropic flow, where the entropy of a fluid is constant along the streamline [79]. The above equation transforms into the following form:

$$u^\mu \nabla_\mu (hu^\nu) + \partial_\nu h = 0. \tag{16}$$

The zeroth component of the above equation gives:

$$\partial_r (hu_t) = 0, \tag{17}$$

Thus, after integrating, we get

$$h\sqrt{\mathcal{F}(r) + (u^r)^2} = C_2, \tag{18}$$

where C_2 is constant. So, both Eqs. (12) and (18) are fundamental equations to describe the matter accretion process across the charged acoustic black hole.

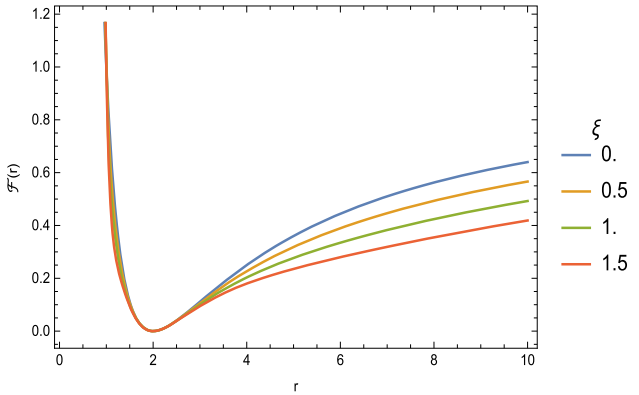

Fig. 1 Display of $\mathcal{F}(r)$ with r with values of $\xi = 0,\ 0.5,\ 1$ and 1.5 from the expression of Eq. (3)

3 Dynamics in Hamiltonian approach

In this section, let us study the concept of sonic points and isothermal test fluid.

- Sonic points: Sonic points are the points around which any dark, compact object achieves its maximum accretion value. At these points, the local speed of sound is always equal to the velocity of infalling matter.

3.1 Speed of sound at sonic points

In the case of charged acoustic black hole metric, Eq. (3), we need to find such sonic points. For that purpose, we take the barotropic fluid at $h = h(n)$ with constant enthalpy [80], thus

$$\frac{dh}{h} = a^2\frac{dn}{n}, \qquad \ln h = a^2 \ln n. \tag{19}$$

Here, a is the local sound speed.

Now, using Eqs. (12), (18) and (19), we have

$$\left[\left(\frac{u^r}{u_t}\right)^2 - a^2\right](\ln u^r)_{,r} = \frac{1}{r(u_t)^2}\left[2a^2(u_t)^2 - \frac{1}{2}r\mathcal{F}'(r)\right]. \tag{20}$$

For the calculation of sonic points, both sides of the above Eq. (20) must be equal to 0. So, it gives

$$a_c^2 = \left(\frac{u_c^r}{u_{tc}}\right)^2, \tag{21}$$

where a_c, r_c and u_c^r are the local sound speed, distance of fluid from the black hole, and velocity of the fluid at sonic point, respectively. Now, the Eq. (20) gives

$$2a_c^2(u_{tc})^2 - \frac{1}{2}r_c\mathcal{F}'(r_c) = 0. \tag{22}$$

Also, following the Eq. (22) with the help of Eq. (21), we have

$$(u_c^r)^2 = \frac{1}{4}r_c\mathcal{F}'(r_c). \tag{23}$$

Again, using Eqs. (10), (22) and (23), we get

$$r_c\mathcal{F}'(r_c) = 4a_c^2[\mathcal{F}(r_c) + (u_c^r)^2], \tag{24}$$

which takes the final form as

$$a_c^2 = \frac{r_c\mathcal{F}'(r_c)}{r_c\mathcal{F}'(r_c) + 4\mathcal{F}(r_c)}. \tag{25}$$

Hence, from Eqs. (23) and (25) we can get the sonic points, $(r_c, \pm u_c^r)$ whenever we put the required value of local sound speed.

3.2 Isothermal test fluids

In the case of isothermal fluids at a constant temperature, during the accretion process, the sonic points of the fluid flow always remain constant. So, this is a very significant step in understanding the accretion process of the acoustic-charged black hole. As matter does not transfer its heat to the surrounding environment due to very high speed (adiabatic situation) let us introduce the adiabatic equation of state $p = \omega e$, where e is the energy density and the state parameter ω follows the condition $0< \omega \leq 1$ [81]. Define $a^2 = \frac{dp}{de}$, $a^2 = \omega$. Now, from the first law of thermodynamics,

$$\frac{de}{dn} = \frac{e+p}{n} = h. \tag{26}$$

If we integrate the Eq. (26), taking the limit from the sonic point to any random point inside the fluid and using $p = ke$, we get

$$n = n_c\left(\frac{e}{e_c}\right)^{\frac{1}{\omega+1}}. \tag{27}$$

So, with the help of the Eq. (14) and the above equation we have the following relation

$$h = \frac{(\omega+1)e_c}{n_c}\left(\frac{n}{n_c}\right)^{\omega}. \tag{28}$$

Thus, by using Eq. (18) and the above equation we get the result as follows

$$n^k\sqrt{\mathcal{F}(r) + (u^r)^2} = C_3 \tag{29}$$

where $C_3 = \frac{C_2 n^{1-\omega}}{(\omega+1)e_c}$.

Again, combining Eqs. (9) and (26) we have

$$\sqrt{\mathcal{F}(r) + (u^r)^2} = C_3 r^{2\omega}(u^r)^{\omega}. \tag{30}$$

Let us consider [79,82] to take the Hamiltonian as follows

$$H = \frac{\mathcal{F}^{1-\omega}}{(1-v^2)^{1-\omega} v^{2\omega} r^{4\omega}}, \tag{31}$$

where $v = \frac{dr}{f dt}$ is 3D speed of radial motion, whose expression is given as

$$v^2 = \left(\frac{u}{f u^t}\right)^2 = \frac{u^2}{u_t^2} = \frac{u^2}{f + u^2}. \tag{32}$$

Finally to get our desired sonic points using Eqs. (23) and (24) we have the following expressions

$$(u_c^r)^2 = \frac{1}{4} r_c \mathcal{F}'(r_c), \tag{33}$$

$$(u_c^r)^2 = \frac{1}{4\omega} r_c \mathcal{F}'(r_c) - \mathcal{F}(r_c). \tag{34}$$

This is the generalized equation of fluid flow, which can be analyzed numerically for different values of the parameter ω within the constraining limits, i.e., for $0 < \omega \leq 1$.

Now, let us consider four different types of fluids: ultra-stiff fluid ($\omega = 1$), ultra-relativistic fluid ($\omega = 1/2$), radiation fluid ($\omega = 1/3$), and sub-relativistic fluid ($\omega = 1/4$) respectively to investigate the accretion process around the charged acoustic black hole.

4 Analysis of charged acoustic black holes for different types of fluids

The solution at the horizon of the black hole metric, Eq. (3) is given by

$$r_{eh} = M + \sqrt{M^2 - Q^2}, \tag{35}$$

$$r_{ch} = M - \sqrt{M^2 - Q^2}, \tag{36}$$

and

$$r_h = \frac{M\xi}{2} \mp \frac{1}{2} M \Xi \mp \frac{1}{2}\sqrt{X_\xi \mp Y_\xi}, \tag{37}$$

where

$$\Xi = \sqrt{\xi^2 - 4\xi}, \tag{38}$$

$$X_\xi = 2M^2\xi^2 - 4M^2\xi - 2\xi Q^2, \tag{39}$$

and

$$Y_\xi = \frac{8M^3\xi^3 - 8M\xi(4M^2\xi + \xi Q^2) + 32M\xi Q^2}{4M\Xi}. \tag{40}$$

Table 1 The sonic points for URF

ξ	r_c	v_c	H_c
0	4.0846	0.135134	0.174527
0.5	2.07854	0.312002	0.1504
1	2.69985	0.385219	0.19167
1.5	2.72399	0.199057	0.29775

provided $\xi \geq 4$.

Next, we follow the four different cases of fluids for the charged acoustic black hole.

4.1 Ultra-stiff fluid

For ultra-stiff fluids ($\omega = 1$), the pressure is the same as the energy density, that is, $p = e$. We find $\mathcal{F}(r_c) = 0$, which gives the critical points at horizons, i.e., r_c = solution of the horizon of BH. The Hamiltonian, given in Eq. (31) reduces to the following form

$$H = \frac{1}{v^2 r^4}. \tag{41}$$

4.2 Ultra-relativistic fluid

In the case of ultra-relativistic fluid, $\omega = 1/2$ implies $p = e/2$, i.e., the pressure becomes less than the energy density. From Eqs. (33) and (34), we have

$$r_c \mathcal{F}'(r_c) - 4\mathcal{F}(r_c) = 0, \tag{42}$$

which gives the following sixth-order polynomial equation in r_c as

$$\begin{aligned} &4r_c^6 - 10Mr_c^5(1+\xi) + r_c^4(48\xi M^2 + 5\xi Q^2 + 6Q^2) \\ &-\xi M r_c^3(48Q^2 + 42M^2) + \xi Q^2 r_c^2(12Q^2 + 84M^2) \\ &-42MQ^4\xi r_c + 7\xi Q^6 = 0. \end{aligned} \tag{43}$$

After getting the value of r_c, we get the value of v_c. Ultimately, we have two critical points like $(r_c, \pm v_c)$. Now, the Hamiltonian, given by Eq. (31) reduces to the following form

$$H = \frac{\sqrt{\mathcal{F}(r)}}{r^2 v\sqrt{1-v^2}}. \tag{44}$$

We have plotted the graph of v with respect to the sonic points in Table 1. Thus, we have

$$v^2 = \frac{H^2 r^4 \pm \sqrt{H^4 r^8 - 4H^2 r^4 \mathcal{F}(r)}}{2H^2 r^4}. \tag{45}$$

Table 2 The sonic points for RF

ξ	r_c	v_c	H_c
0	3.99599	0.980634	0.557103
0.5	4.90282	0.984200	0.55996
1	5.47132	0.987826	0.567354
1.5	6.03312	0.991258	0.58534

Table 3 The sonic points for SRF

ξ	r_c	v_c	H_c
0	4.99666	0.954645	0.95713
0.5	5.80417	0.947816	0.76952
1	7.19507	0.9505	0.66359
1.5	9.40923	0.944731	0.47655

4.3 Radiation fluid

In the case of the radiation fluid, $\omega = 1/3$ implies $p = e/3$. From Eqs. (33) and (34), we have the real solution in the following form

$$r_c\mathcal{F}'(r_c) - 2\mathcal{F}(r_c) = 0, \tag{46}$$

giving the final form of solution as follows

$$\begin{aligned} &2r_c^6 - 6Mr_c^5(1+\xi) + r_c^4(32\xi M^2 + 3\xi Q^2 + 4Q^2) \\ &- \xi M r_c^3(36Q^2 + 40M^2) + \xi Q^2 r_c^2(8Q^2 + 52M^2) \\ &- 30MQ^4\xi r_c + 5\xi Q^6 = 0. \end{aligned} \tag{47}$$

The Hamiltonian, given by Eq. (31) reduces to the following form

$$H = \frac{\mathcal{F}(r)^{2/3}}{r^{4/3}v^{2/3}(1-v^2)^{2/3}}. \tag{48}$$

We have plotted the graph of v with respect to sonic points of Table 2 with the help of the given equation

$$H^3r^4v^6 - 2H^3r^4v^4 + H^3r^4v^2 - \mathcal{F}(r)^2 = 0. \tag{49}$$

4.4 Sub-relativistic fluid

In the case of the radiation fluid, $\omega = 1/4$ implies $p = e/4$. From Eqs. (33) and (34), we have the real solution as follows

$$4\mathcal{F}(r)r_c - 3\mathcal{F}'(r_c) = 0, \tag{50}$$

giving the final form of the solution as below

$$\begin{aligned} &4r_c^6 - 14Mr_c^5(1+\xi) + r_c^4(60\xi M^2 + 7\xi Q^2 + 10Q^2) \\ &-\xi M r_c^3(70Q^2 + 64M^2) + \xi Q^2 r^2(21Q^2 + 116M^2) \\ &-68MQ^4\xi r_c + 13\xi Q^6 = 0. \end{aligned} \tag{51}$$

The Hamiltonian in Eq. (31) reduces to

$$H = \frac{\mathcal{F}(r)^{3/4}}{rv^{1/2}(1-v^2)^{3/4}}. \tag{52}$$

We have plotted the graph of v with respect to sonic points of Table 3 with the help of the given equation

$$H^4r^4v^8 - 3H^4r^4v^6 + 3H^4r^4v^4 - H^4r^4v^2 + \mathcal{F}(r)^3 = 0. \tag{53}$$

5 Result analysis of all different types of fluids

In this section, let us explain all the results for ultra-stiff fluids, ultra-relativistic fluids, radiation fluids, and sub-relativistic fluids for the acoustic-charged black hole, respectively, in a detailed manner.

5.1 Ultra-stiff fluid with charged black hole

The sonic accretion for the ultra-stiff fluid is depicted in Fig. 2 with the help of Eq. (31). We have perceived the outward motion from the horizon (supersonic accretion) in the region $v > 0$ and the inward motion towards the horizon (subsonic accretion) in the region $v < 0$ of this type of fluid in Fig. 2. We have then noticed the scenario of the passing of curves through the critical points $(r_c, \pm v_c)$. We also have the pictorial form of the streamlines of this fluid accretion.

5.2 Ultra-relativistic fluid with charged black hole

The sonic accretion for the ultra-relativistic fluid is depicted in Fig. 3 with the help of Eq. (44) with respect to Table 1. Associated with the critical point $(r_c, \pm v_c)$, we have perceived the supersonic fluid motion in the region $v > v_c$ on the edge of the horizon and the subsonic fluid motion in the region $v < v_c$ away from the horizon in Fig. 3. We have then noticed the scenario of the passing of curves through the critical points $(r_c, \pm v_c)$. We also have the pictorial form of the streamlines of this fluid accretion.

5.3 Radiation fluid with charged black hole

The sonic accretion for the radiation fluid is depicted in Fig. 4 with the help of Eq. (48) with respect to Table 2. Associated with the critical point $(r_c, \pm v_c)$, we have perceived the supersonic fluid motion in the region $v > v_c$ away from the horizon and the subsonic fluid motion in the region $v < v_c$ away from the horizon in Fig. 4. We have then noticed the scenario of the passing of curves through the critical points

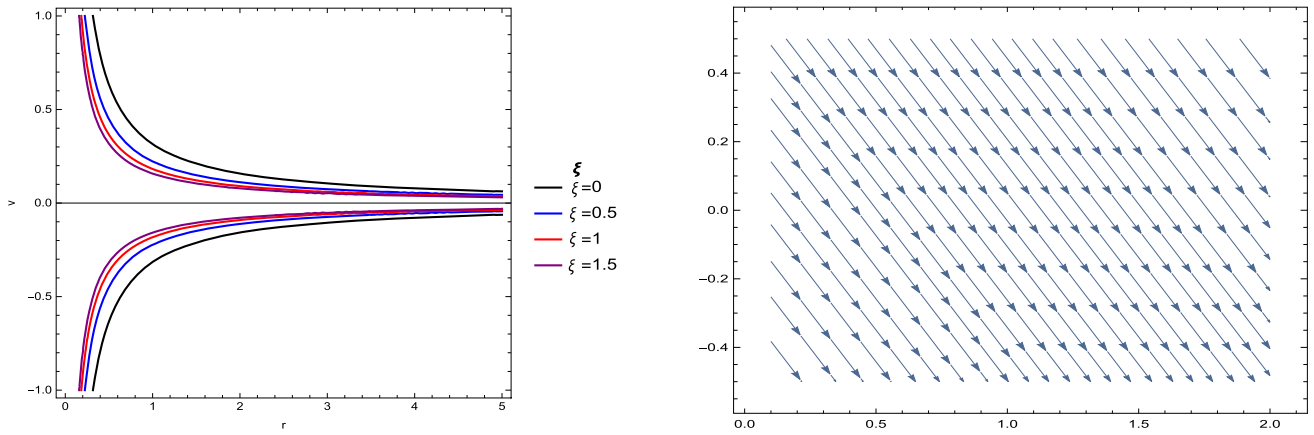

Fig. 2 Accretion display of ultra-stiff fluid with the variation of H_c for $\xi = 0, 0.5, 1, 1.5$ corresponding to black, blue, red, and purple and the representation of the streamlines accretion

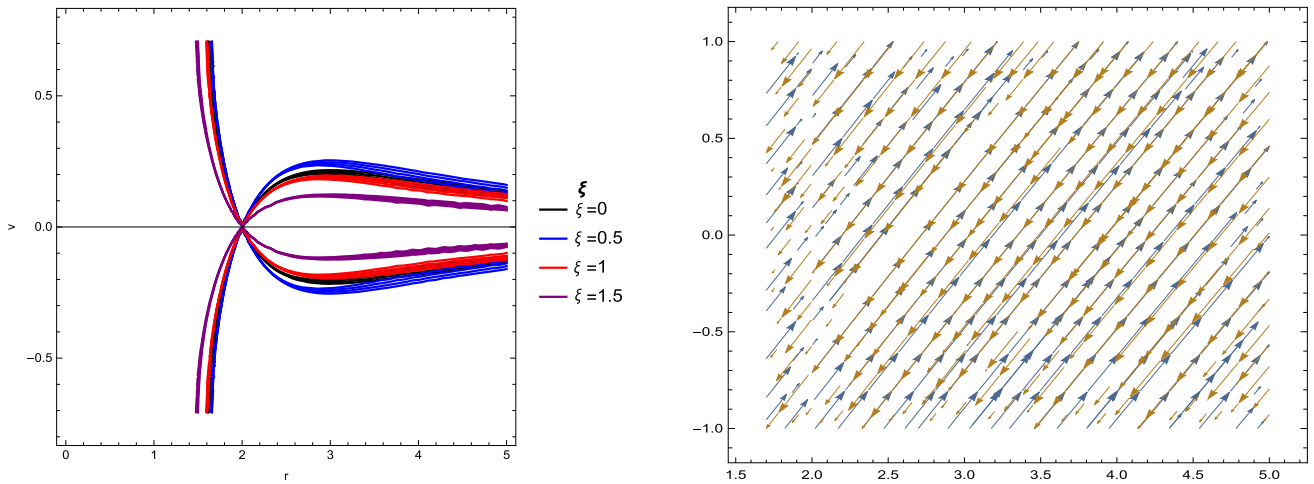

Fig. 3 Accretion display of ultra-relativistic fluid with the variation of H_c from Table 1 for ξ=0, 0.5, 1, 1.5 corresponding to black, blue, red, and purple and the representation of the streamlines accretion

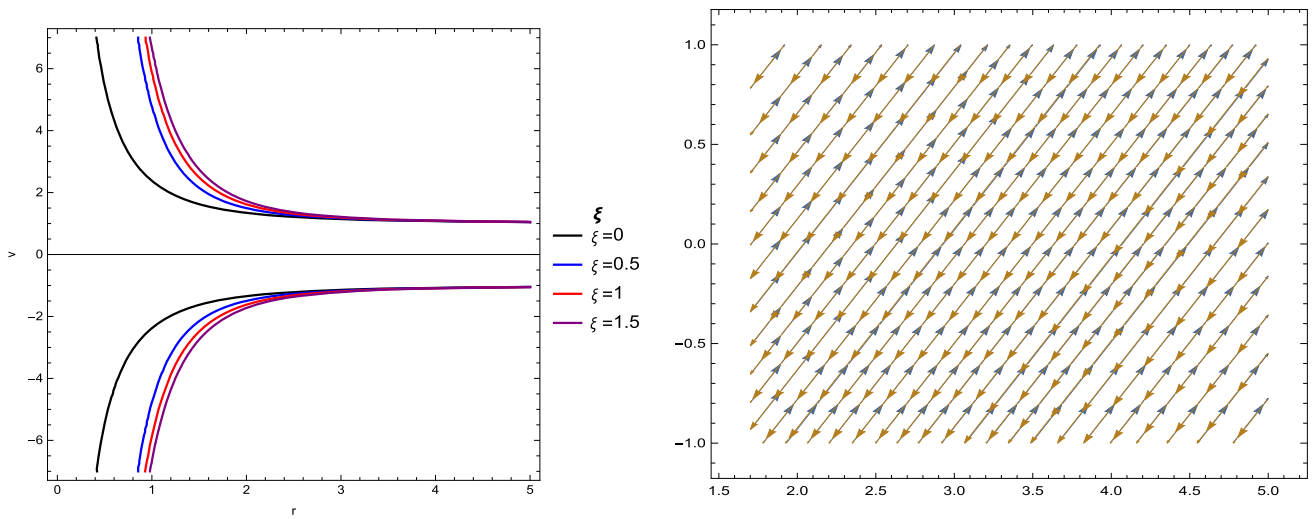

Fig. 4 Accretion display of radiation fluid with the variation of H_c from Table 2 for ξ=0, 0.5, 1, 1.5 corresponding to black, blue, red, and purple and the representation of the streamlines accretion

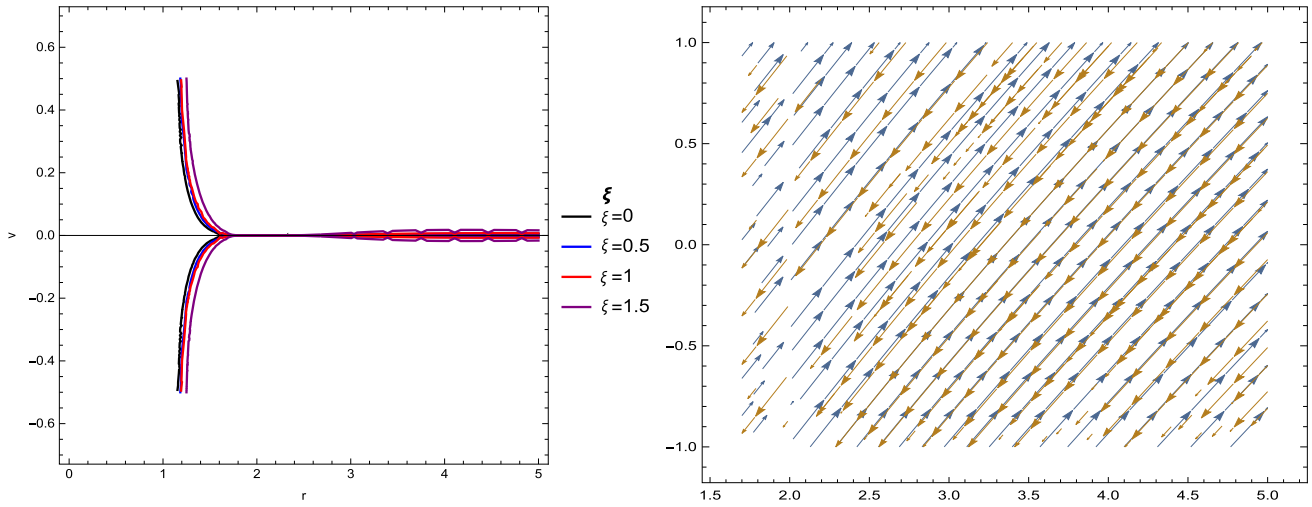

Fig. 5 Accretion display of sub-relativistic fluid with the variation of H_c from Table 3 for ξ =0, 0.5, 1, 1.5 corresponding to black, blue, red, and purple and the representation of the streamlines accretion

$(r_c, \pm v_c)$. We also have the pictorial form of the streamlines of this fluid accretion.

5.4 Sub-relativistic fluid with charged black hole

The sonic accretion for the sub-relativistic fluid is depicted in Fig. 5 with the help of Eq. (52) with respect to Table 3. Associated with the critical point $(r_c, \pm v_c)$, we have perceived the supersonic fluid motion in the region $v > v_c$ away from the horizon and the subsonic fluid motion in the region $v < v_c$ away from the horizon in Fig. 5. We have then noticed the scenario of the passing of curves through the critical points $(r_c, \pm v_c)$. We also have the pictorial form of the streamlines of this fluid accretion.

6 Rate of accretion flow of black hole

This section is devoted to measuring the rate of accretion flow of four fluids around the acoustic-charged black hole with the effect of radius. We have the energy–momentum tensor for the perfect fluid as $T_t^r = (e + p)u_t u^r$ [9,65]. The conservation of the dynamical system is given by $\nabla_\mu J^\mu = 0$ and $\nabla_\nu T^{\mu\nu} = 0$.

Next, we presume the general form of the rate of mass accretion of black hole [83]

$$\dot{M}|_{r_h} = 4\pi r^2 T_t^r|_{r_h}. \tag{54}$$

Using the above conservation laws with Eqs. (12) and (18), we have

$$r^2 u^r (e + p)\sqrt{\mathcal{F}(r) + (u^r)^2} = A_0, \tag{55}$$

where A_0 is an arbitrary constant.

The equation of continuity, or we can say the equation of relativistic energy flux together with the equation of state, gives the following relation

$$\frac{de}{e + p} + \frac{du^r}{u^r} + \frac{2}{r}dr = 0. \tag{56}$$

Upon integration, it transforms into

$$r^2 u^r exp\left[\int_{e_\infty}^{e} \frac{de'}{e' + p(e')}\right] = -A_1, \tag{57}$$

where A_1 is a integrating constant and e_∞ denotes the fluid density at the infinity. The minus sign on the right-hand side of the Eq. (57) denotes the inward flow of fluid to the black hole as $u^r < 0$.

With the account of Eqs. (57) and (55), we get

$$A_3 = -\frac{A_0}{A_1} = (e + p)\sqrt{\mathcal{F}(r) + (u^r)^2} exp\left[-\int_{e_\infty}^{e} \frac{de'}{e' + p(e')}\right], \tag{58}$$

where A_3 denotes the integration constant, and the boundary value for the infinity is given as $A_3 = e_\infty + p(e_\infty) = -\frac{A_0}{A_1}$ with $A_0 = (e + p)u^t u^r r^2 = -A_1(e_\infty + p(e_\infty))$. As per spherical symmetric on the equatorial plane, the mass flux is given by

$$r^2 u^r n = A_2, \tag{59}$$

A_2 being the constant.

Next, from Eqs. (55) and (59), we have

$$\frac{e+p}{n}\sqrt{\mathcal{F}(r)+(u^r)^2}=\frac{A_0}{A_2}=A_4, \tag{60}$$

where the constant $A_4=\frac{e_\infty+p_\infty}{n_\infty}$.

Next, putting Eq. (55) into Eq. (54), the mass accretion rate of flow onto the black hole is given by

$$\dot{M}=-4\pi r^2u^r(e+p)\sqrt{\mathcal{F}(r)+(u^r)^2}=-4\pi A_0, \tag{61}$$

simplifying to

$$\dot{M}=4\pi A_1\left(e_\infty+p(e_\infty)\right). \tag{62}$$

which depicts the validity of various types of fluids. Now, the mass accretion rate of the black hole becomes

$$\dot{M}=4\pi A_1(e+p)|_{r_h}. \tag{63}$$

With the account of $p=\omega e$, Eq. (57) leads to the result

$$e=\left[-\frac{A_1}{r^2u^r}\right]^{\omega+1}. \tag{64}$$

- **Mass accretion rate of ultra-stiff fluid:** In this case, by putting $\omega=1$, we have the corresponding equation in u^r using Eqs. (55) and (64) as follows

$$\left(u^r\right)^2\left(4A_1^4-A_0^2\right)+4A_1^4\mathcal{F}(r)=0, \tag{65}$$

After solving we get

$$u^r=\pm2A_1^2\frac{\sqrt{\mathcal{F}(r)}}{\sqrt{A_0^2-4A_1^4}}. \tag{66}$$

and using this with Eq. (64), we obtain

$$e=\frac{\left(A_0^2-4A_1^4\right)^2}{16A_1^6r^4\mathcal{F}(r)^2}. \tag{67}$$

Finally, putting the value of this e in Eq. (63), we get the accretion rate of the charged acoustic black hole as

$$\dot{M}=\frac{\pi\left(A_0^2-4A_1^4\right)^2}{2A_1^5r^4\mathcal{F}(r)^2}. \tag{68}$$

From Fig. 6a, we see the accretion rate with r. As r increases, the rate of mass first remains fixed and then rapidly increases for different values of ω. For $\omega=0$, the rate of mass increases gradually with respect to radius. But as ω increases, at first, the rate of mass remains fixed, and after a certain radius, it rapidly increases as r tends to a higher value.

- **Mass accretion rate of ultra-relativistic fluid:** In this case, by putting $\omega=1/2$, we have the corresponding equation in u^r using Eqs. (55) and (64) as below

$$9A_1^3\left(u^r\right)^2-4r^2A_0^2u^r+9A_1^3\mathcal{F}(r)=0, \tag{69}$$

After solving we get

$$u^r=\frac{2r^2A_0^2\pm\sqrt{4r^4A_0^4-81A_1^6\mathcal{F}(r)}}{9A_1^3}. \tag{70}$$

and using this with Eq. (64), we obtain

$$e=\left[-\frac{9A_1^4}{r^2\left(2r^2A_0^2\pm\sqrt{4r^4A_0^4-81A_1^6\mathcal{F}(r)}\right)}\right]^{3/2}. \tag{71}$$

Finally, putting this value of e into the Eq. (63), we get the accretion rate of our black hole as

$$\dot{M}=6\pi A_1\left[-\frac{9A_1^4}{r^2\left(2r^2A_0^2\pm\sqrt{4r^4A_0^4-81A_1^6\mathcal{F}(r)}\right)}\right]^{3/2}. \tag{72}$$

From Fig. 6b, we see the accretion rate with r. As r increases, the rate of mass first remains fixed and then rapidly increases for different values of ω. As ω increases, at first, the rate of mass remains fixed, and after a certain radius, it gets rapid increment as r tends to a higher value.

- **Mass accretion rate of radiation fluid:** In this case, by putting $\omega=1/3$, we have the corresponding equation in u^r using Eqs. (55) and (64) as follows

$$\begin{aligned}&4096A_1^8\left(u^r\right)^6+12288A_1^8\mathcal{F}(r)\left(u^r\right)^4\\&+\left(12288A_1^8\mathcal{F}(r)^2-729A_0^6r^4\right)\left(u^r\right)^2\\&+4096A_1^8\mathcal{F}(r)^3=0,\end{aligned} \tag{73}$$

After solving from Eqs. (64) and (63) we can obtain e and $\dot{M}$.

From Fig. 7a, we see the accretion rate with r. As r increases, the rate of mass first rapidly decreases and then remains fixed for different values of ω. As ω increases, at first, the rate of mass rapidly decreases and then remains fixed after a certain radius as r tends to a higher value.

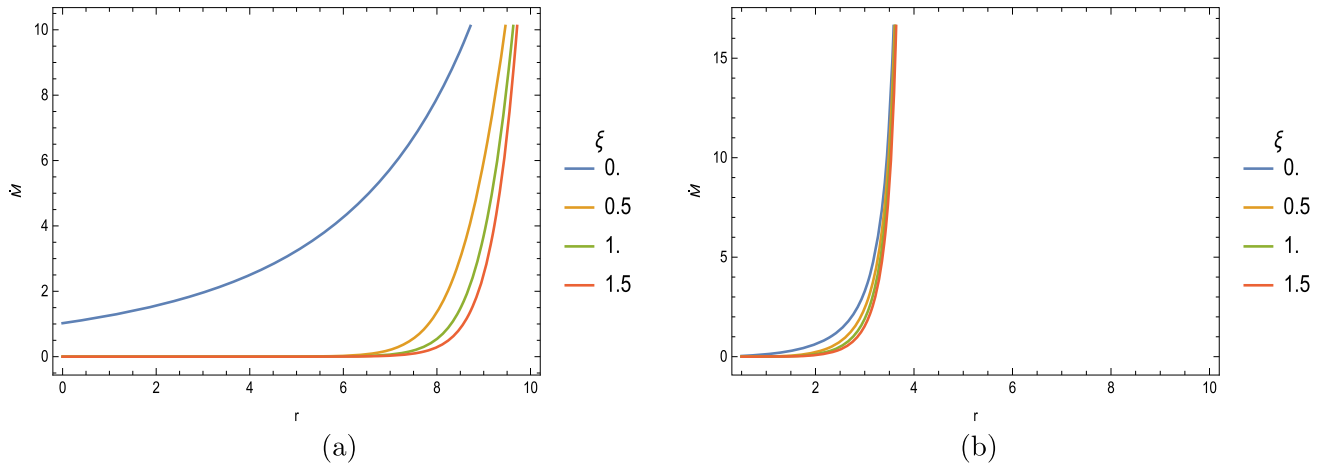

Fig. 6 Display of accretion rate of mass around the acoustic charged black hole for ultra-stiff fluid and ultra-relativistic fluid, respectively, with respect to r for different values of ω and with the variation of H_0 from Table 1 for ξ =0, 0.5, 1, 1.5

- **Mass accretion rate of sub-relativistic fluid:** In this case, by putting $\omega = 1/4$, we have the corresponding equation in u^r using Eqs. (55) and (64) as below

$$625A_1^5\left(u^r\right)^4 + 1250A_1^5\mathcal{F}(r)\left(u^r\right)^2 + 256r^2A_0^4u^r + 625A_1^5\mathcal{F}(r)^2 = 0, \tag{74}$$

After solving from Eqs. (64) and (63) we can obtain e and $\dot{M}$.

From Fig. 7b, we see the accretion rate with r. As r increases, the rate of mass first rapidly decreases and then remains fixed for different values of ω. When $\omega = 0$, the rate of mass decreases gradually with r. As ω increases, at first, the rate of mass rapidly decreases and then remains fixed after a certain radius as r tends to a higher value.

7 Inference

In this accelerating universe, black holes are still one of the puzzling objects that attract researchers' attention. Although it has very few physical properties, mass, charge, and angular momentum are the only three things that can help us identify a black hole at its basic level. This paper is dedicated to examining the acoustic-charged black hole in the background of Gross–Pitaevskii theory [39,43,77], which starts with a complex scalar field. Then, on account of the Klein–Gordon equation, some relativistic equations of phase fluctuation have been governed to have an effective metric with four velocity components. This black hole metric has been derived with an interesting tuning parameter ξ. For the higher value of this parameter, this black hole acquires the infinite value of the escape velocity. This also implies the infiniteness of the event horizon of this black hole. After taking the analysis of its horizon structures, we got a total of six solutions for the horizons of this black hole together with the extremal case.

For our proposed acoustic-charged black hole, we have gone through an analysis of matter accretion of the test particles with acceleration. To find some physical aspects, we have considered different kinds of fluid. Using Hamiltonian principles, our investigation of the accretion process around the acoustic-charged black hole has been followed as below:

- As per discussion in Sect. 2, the horizon structures of our proposed black hole have been prospected depending on the different values of the tuning parameter ξ. According to Fig. 1, we have seen the physical behavior of the horizon structures with the values of $\xi = 0, 0.5, 1, 1.5$ for our BH solution.
- Next, in Sect. 3, we have produced the accretion process to explore the accretion fluid flow having some fundamental aspects around the acoustic charged black hole. We have also gone through the Hamiltonian approach to have sonic points. The isothermal test fluid method has been deliberated about the formulation of the expressions, given by Eqs. (33) and (34) to look into the sonic points for our proposed acoustic charged BH.
- Four different types of fluid, such as ultra-stiff fluid, ultra-relativistic fluid, radiation fluid, and sub-relativistic fluid with $w = 1,\ 1/2,\ 1/3$ and $1/4$ respectively, have been contemplated to portray the scenario of the accretion flow around the acoustic charged BH. For every case of these four fluids, the critical points have been calculated using the expressions given by Eqs. (33) and (34).
- The sonic accretion for the ultra-stiff fluid has been portrayed in Fig. 2 with the help of Eq. (31). We have perceived the outward motion from the horizon (supersonic accretion) in the region $v > 0$ and the inward motion towards the horizon (subsonic accretion) in the region

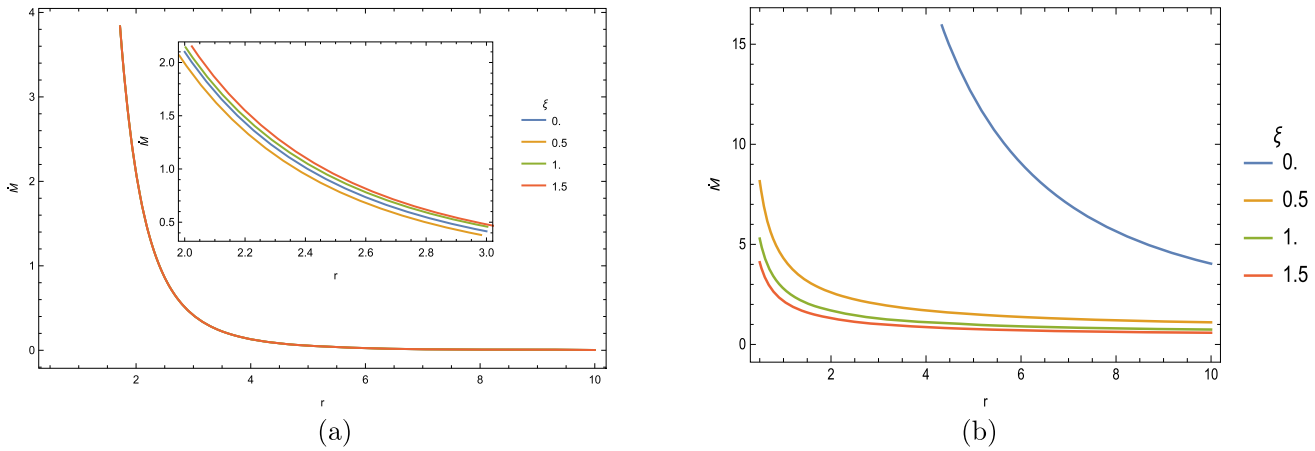

Fig. 7 Display of accretion rate of mass around the acoustic charged black hole for radiation fluid and sub-relativistic fluid, respectively, with respect to r for different values of ω and with the variation of H_0 from Tables 2 and 3 for ξ =0, 0.5, 1, 1.5

$v < 0$ of this type of fluid in Fig. 2. We have then noticed the scenario of the passing of curves through the critical points $(r_c, \pm v_c)$. We also have the pictorial form of the streamlines of this fluid accretion.

- The sonic accretion for the ultra-relativistic fluid has been portrayed in Fig. 3 with the help of Eq. (44) with respect to Table 1. Associated to critical point $(r_c, \pm v_c)$, we have perceived the supersonic fluid motion in the region $v > v_c$ on the verge of the horizon and the subsonic fluid motion in the region $v < v_c$ away from the horizon in Fig. 3. We have then noticed the scenario of the passing of curves through the critical points $(r_c, \pm v_c)$. We also have the pictorial form of the streamlines of this fluid accretion.
- The sonic accretion for the radiation fluid has been portrayed in Fig. 4 with the help of Eq. (48) with respect to Table 2. Associated to critical point $(r_c, \pm v_c)$, we have perceived the supersonic fluid motion in the region $v > v_c$ away from the horizon and the subsonic fluid motion in the region $v < v_c$ on the verge of the horizon in Fig. 4. We have then noticed the scenario of the passing of curves through the critical points $(r_c, \pm v_c)$. We also have the pictorial form of the streamlines of this fluid accretion.
- The sonic accretion for the radiation fluid has been portrayed in Fig. 5 with the help of Eq. (52) with respect to Table 3. Associated to critical point $(r_c, \pm v_c)$, we have perceived the supersonic fluid motion in the region $v > v_c$ away from the horizon and the subsonic fluid motion in the region $v < v_c$ on the verge of the horizon in Fig. 5. We have then noticed the scenario of the passing of curves through the critical points $(r_c, \pm v_c)$. We also have the pictorial form of the streamlines of this fluid accretion.
- The pictures of mass accretion rates for ultra-stiff fluid, ultra-relativistic fluid, radiation fluid, and sub-relativistic fluid around the acoustic charged black hole have been displayed in Figs. 6 and 7 respectively. For ultra-stiff fluid and ultra-relativistic fluid, we have seen that as ω increases, at first, the rate of mass remains fixed, and after a certain radius, it rapidly increases as r tends to a higher value. Next, in the case of radiation fluid and sub-relativistic fluid, as ω increases, at first, the rate of mass rapidly decreases and then remains fixed after a certain radius as r tends to a higher value.

Overall, in this study, we have gone through the accretion investigation of different types of fluid like ultra-stiff fluid, ultra-relativistic fluid, radiation fluid, and sub-relativistic fluid around the acoustic charged black hole with the analysis of the horizon structure by the influence of [59,63,66,74]. With the variation of the tuning parameter ξ, we have analyzed the physical properties as well as sonic points of these multiple fluids around our proposed BH. By investigating the accretion rate of these fluids, we have revealed some stable and reliable results that are compatible with the observational data.

Acknowledgements PM is grateful for providing an Institute Fellowship [SRF] to the Indian Institute of Engineering Science and Technology, Shibpur, India. PS acknowledges Government of West Bengal Science and Technology and Biotechnology Department, for financial support to carry out Research project No.: STBT-11012(31)/5/2024-WBSCST SEC.

Data Availability Statement This manuscript has no associated data. [Authors' comment: This is a theoretical study with no experimental data.]

Code Availability Statement This manuscript has no associated code/software. [Authors' comment: Code/Software sharing is not appli-

cable to this article since no code or software was generated or analyzed in this study.]

Funded by SCOAP[3].

References

1. P.M. Garnavich, R.P. Kirshner, P. Challis et al., Constraints on cosmological models from Hubble Space Telescope observations of high-z supernovae. Astrophys. J. **493**(2), L53 (1998). https://doi.org/10.1086/311140
2. N.A. Bahcall, J.P. Ostriker, S. Perlmutter, P.J. Steinhardt, The cosmic triangle: revealing the state of the universe. Science **284**(5419), 1481–1488 (1999). https://doi.org/10.1126/science.284.5419.1481
3. S. Perlmutter, G. Aldering, G. Goldhaber et al., Measurements of Ω and Λ from 42 high-redshift supernovae. Astrophys. J. **517**(2), 565 (1999). https://doi.org/10.1086/307221
4. S. Allen, R.W. Schmidt, H. Ebeling, A. Fabian, L. Van Speybroeck, Constraints on dark energy from Chandra observations of the largest relaxed galaxy clusters. Mon. Not. R. Astron. Soc. **353**(2), 457–467 (2004). https://doi.org/10.1111/j.1365-2966.2004.08080.x
5. R. Adam, P.A. Ade, N. Aghanim et al., Planck 2015 results-I. Overview of products and scientific results. Astron. Astrophys. **594**, A1 (2016). https://doi.org/10.1051/0004-6361/201527101
6. D.N. Spergel, R. Bean, O. Doré et al., Three-year Wilkinson Microwave Anisotropy Probe (WMAP) observations: implications for cosmology. Astrophys. J. Suppl. Ser. **170**(2), 377 (2007). https://doi.org/10.1086/513700
7. D.J. Eisenstein, I. Zehavi, D.W. Hogg et al., Detection of the baryon acoustic peak in the large-scale correlation function of SDSS luminous red galaxies. Astrophys. J. **633**(2), 560 (2005). https://doi.org/10.1086/466512
8. D.N. Spergel, L. Verde, H.V. Peiris et al., First-year Wilkinson Microwave Anisotropy Probe (WMAP)* observations: determination of cosmological parameters. Astrophys. J. Suppl. Ser. **148**(1), 175 (2003). https://doi.org/10.1086/377226
9. M. Jamil, A. Qadir, M.A. Rashid, Charged black holes in phantom cosmology. Eur. Phys. J. C **58**, 325–329 (2008). https://doi.org/10.1140/epjc/s10052-008-0761-9
10. M. Sharif, G. Abbas, Phantom energy accretion by a stringy charged black hole. Chin. Phys. Lett. **29**(1), 010 401 (2012). https://doi.org/10.1088/0256-307X/29/1/010401
11. G. Mustafa, F. Javed, A. Ditta, S. Maurya, Y. Liu, F. Atamurotov, Matter accretion onto charged black holes in symmergent gravity. Phys. Dark Univ. **42**, 101–376 (2023). https://doi.org/10.1016/j.dark.2023.101376
12. G. Abbas, A. Ditta, Accretion onto a charged Kiselev black hole. Mod. Phys. Lett. A **33**(13), 1 850 070 (2018). https://doi.org/10.1142/S0217732318500700
13. M. Sharif, S. Iftikhar, Accretion onto a charged higher-dimensional black hole. Eur. Phys. J. C **76**, 1–8 (2016). https://doi.org/10.1140/epjc/s10052-016-4001-4
14. H. Rehman, G. Abbas, T. Zhu, G. Mustafa, Matter accretion onto the magnetically charged Euler–Heisenberg black hole with scalar hair. Eur. Phys. J. C **83**(9), 1–16 (2023). https://doi.org/10.1140/epjc/s10052-023-12033-5
15. W.G. Unruh, Experimental black-hole evaporation? Phys. Rev. Lett. **46**(21), 1351 (1981). https://doi.org/10.1103/PhysRevLett.46.1351
16. M. Visser, Acoustic black holes: horizons, ergospheres and Hawking radiation. Class. Quantum Gravity **15**(6), 1767 (1998). https://doi.org/10.1088/0264-9381/15/6/024
17. V. Cardoso, J.P. Lemos, S. Yoshida, Quasinormal modes and stability of the rotating acoustic black hole: numerical analysis. Phys. Rev. D Part. Fields Gravit. Cosmol. **70**(12), 124 032 (2004). https://doi.org/10.1103/PhysRevD.70.124032
18. C.L. Benone, L.C. Crispino, C. Herdeiro, E. Radu, Acoustic clouds: standing sound waves around a black hole analogue. Phys. Rev. D **91**(10), 104 038 (2015). https://doi.org/10.1103/PhysRevD.91.104038
19. S. Sarkar, A. Bhattacharyay, Quantum potential induced UV-IR coupling in analogue Hawking radiation: from Bose–Einstein condensates to canonical acoustic black holes. Phys. Rev. D **96**(6), 064 027 (2017). https://doi.org/10.1103/PhysRevD.96.064027
20. S. Liberati, G. Tricella, A. Trombettoni, Back-reaction in canonical analogue black holes. Appl. Sci. **10**(24), 8868 (2020). https://doi.org/10.3390/app10248868
21. H. Vieira, V. Bezerra, Acoustic black holes: massless scalar field analytic solutions and analogue Hawking radiation. Gen. Relativ. Gravit. **48**, 1–20 (2016). https://doi.org/10.1007/s10714-016-2082-x
22. H. Nakano, Y. Kurita, K. Ogawa, C.-M. Yoo, Quasinormal ringing for acoustic black holes at low temperature. Phys. Rev. D Part. Fields Gravit. Cosmol. **71**(8), 084 006 (2005). https://doi.org/10.1103/PhysRevD.71.084006
23. C. Barcelo, S. Liberati, M. Visser, Analogue gravity. Living Rev. Relativ. **14**, 1–159 (2011). https://doi.org/10.12942/lrr-2005-12
24. E. Berti, V. Cardoso, J.P. Lemos, Quasinormal modes and classical wave propagation in analogue black holes. Phys. Rev. D Part. Fields Gravit. Cosmol. **70**(12), 124 006 (2004). https://doi.org/10.1103/PhysRevD.70.124006
25. C. Song-Bai, J. Ji-Liang, Quasinormal modes of a coupled scalar field in the acoustic black hole spacetime. Chin. Phys. Lett. **23**(1), 21 (2006). https://doi.org/10.1088/0256-307X/23/1/007
26. M. Anacleto, F. Brito, C. Garcia, G. Luna, E. Passos, Quantum-corrected rotating acoustic black holes in Lorentz-violating background. Phys. Rev. D **100**(10), 105 005 (2019). https://doi.org/10.1103/PhysRevD.100.105005
27. R. Balbinot, A. Fabbri, R.A. Dudley, P.R. Anderson, Particle production in the interiors of acoustic black holes. Phys. Rev. D **100**(10), 105 021 (2019). https://doi.org/10.1103/PhysRevD.100.105021
28. G. Eskin, New examples of Hawking radiation from acoustic black holes (2019). https://doi.org/10.48550/arXiv.1906.06038. arXiv:1906.06038
29. G. Eskin, Hawking type radiation from acoustic black holes with time-dependent metric. Rep. Math. Phys. **88**(2), 161–174 (2021). https://doi.org/10.1016/S0034-4877(21)00067-7
30. B. Zhang, Thermodynamics of acoustic black holes in two dimensions. Adv. High Energy Phys. **2016**(1), 5 710 625 (2016). https://doi.org/10.1155/2016/5710625
31. Q.-B. Wang, X.-H. Ge, Geometry outside of acoustic black holes in (2+ 1)-dimensional spacetime. Phys. Rev. D **102**(10), 104 009 (2020). https://doi.org/10.1103/PhysRevD.102.104009

32. M. Isoard, N. Pavloff, Departing from thermality of analogue Hawking radiation in a Bose–Einstein condensate. Phys. Rev. Lett. **124**(6), 060 401 (2020). https://doi.org/10.1103/PhysRevLett.124.060401
33. M. Visser, Acoustic black holes (1999). https://doi.org/10.48550/arXiv.gr-qc/9901047. arXiv:gr-qc/9901047
34. X.-H. Ge, S.-J. Sin, Acoustic black holes for relativistic fluids. J. High Energy Phys. **2010**(6), 1–16 (2010). https://doi.org/10.1007/JHEP06(2010)087
35. X.-H. Ge, S.-F. Wu, Y. Wang, G.-H. Yang, Y.-G. Shen, Acoustic black holes from supercurrent tunneling. Int. J. Mod. Phys. D **21**(04), 1 250 038 (2012). https://doi.org/10.1142/S0218271812500381
36. M. Anacleto, F. Brito, E. Passos, Acoustic black holes from Abelian Higgs model with Lorentz symmetry breaking. Phys. Lett. B **694**(2), 149–157 (2010). https://doi.org/10.1016/j.physletb.2010.09.045
37. M. Anacleto, F. Brito, E. Passos, Supersonic velocities in noncommutative acoustic black holes. Phys. Rev. D Part. Fields Gravit. Cosmol. **85**(2), 025 013 (2012). https://doi.org/10.1103/PhysRevD.85.025013
38. X.-H. Ge, J.-R. Sun, Y. Tian, X.-N. Wu, Y.-L. Zhang, Holographic interpretation of acoustic black holes. Phys. Rev. D **92**(8), 084 052 (2015). https://doi.org/10.1103/PhysRevD.92.084052
39. X.-H. Ge, M. Nakahara, S.-J. Sin, Y. Tian, S.-F. Wu, Acoustic black holes in curved spacetime and the emergence of analogue Minkowski spacetime. Phys. Rev. D **99**(10), 104 047 (2019). https://doi.org/10.1103/PhysRevD.99.104047
40. B. Toshmatov, A. Abdukarimov, Frequency shift of photon radiated from accretion disc of acoustic black hole. Ann. Phys. **440**, 168 845 (2022). https://doi.org/10.1016/j.aop.2022.168845
41. H. Vieira, K.D. Kokkotas, Quasibound states of Schwarzschild acoustic black holes. Phys. Rev. D **104**(2), 024 035 (2021). https://doi.org/10.1103/PhysRevD.104.024035
42. H. Guo, H. Liu, X.-M. Kuang, B. Wang, Acoustic black hole in Schwarzschild spacetime: quasinormal modes, analogous Hawking radiation, and shadows. Phys. Rev. D **102**(12), 124 019 (2020). https://doi.org/10.1103/PhysRevD.102.124019
43. R. Ling, H. Guo, H. Liu, X.-M. Kuang, B. Wang, Shadow and near-horizon characteristics of the acoustic charged black hole in curved spacetime. Phys. Rev. D **104**(10), 104 003 (2021). https://doi.org/10.1103/PhysRevD.104.104003
44. D. Mondal, U. Debnath, A. Pradhan, Thermodynamics of charged acoustic black hole: heat engine. Int. J. Geom. Methods Mod. Phys. (2024). https://doi.org/10.1142/S0219887825300028
45. H. Bondi, On spherically symmetrical accretion. Mon. Not. R. Astron. Soc. **112**(2), 195–204 (1952). https://doi.org/10.1093/mnras/112.2.195
46. F.C. Michel, Accretion of matter by condensed objects. Astrophys. Space Sci. **15**, 153–160 (1972). https://doi.org/10.1007/BF00649949
47. M. Begelman, Accretion of gamma 5/3 gas by a Schwarzschild black hole (1978)
48. E. Bettwieser, W. Glatzel, On the growth of primordial black holes. Astron. Astrophys. **94**(2), 306–312 (1981). (**Deutsche Forschungsgemeinschaft, vol. 94, pp. 306–312 (1981)**)
49. S.L. Shapiro, S.A. Teukolsky, B. Holes, W. Dwarfs, N. Stars, *The Physics of Compact Objects*, vol. 19832 (Wiley, New York, 1983), pp. 119–123
50. L.I. Petrich, S.L. Shapiro, S.A. Teukolsky, Accretion onto a moving black hole: an exact solution. Phys. Rev. Lett. **60**(18), 1781 (1988). https://doi.org/10.1103/PhysRevLett.60.1781
51. E. Malec, Fluid accretion onto a spherical black hole: relativistic description versus the Bondi model. Phys. Rev. D **60**(10), 104 043 (1999). https://doi.org/10.1103/PhysRevD.60.104043
52. J. Karkowski, B. Kinasiewicz, P. Mach, E. Malec, Z. Świerczyński, Universality and backreaction in a general-relativistic accretion of steady fluids. Phys. Rev. D Part. Fields Gravit. Cosmol. **73**(2), 021 503 (2006). https://doi.org/10.1103/PhysRevD.73.021503
53. E. Babichev, V. Dokuchaev, Y. Eroshenko, Black hole mass decreasing due to phantom energy accretion. Phys. Rev. Lett. **93**(2), 021 102 (2004). https://doi.org/10.1103/PhysRevLett.93.021102
54. E. Babichev, V. Dokuchaev, Y.N. Eroshenko, The accretion of dark energy onto a black hole. J. Exp. Theor. Phys. **100**, 528–538 (2005). https://doi.org/10.1134/1.1901765
55. P. Mukherjee, U. Debnath, A. Pradhan, Accretion of modified Chaplygin–Jacobi gas and modified Chaplygin–Abel gas onto Schwarzschild black hole. Int. J. Geom. Methods Mod. Phys. **20**(12), 2 350 218 (2023). https://doi.org/10.1142/S0219887823502183
56. G. Mustafa, A. Ditta, F. Javed, S.K. Maurya, H. Chaudhary, F. Atamurotov, A study on matter accretion onto charged black hole solution in metric-affine gravity. Chin. J. Phys. **89**, 628–648 (2024). https://doi.org/10.1016/j.cjph.2024.03.034
57. A. Majumdar, Domination of black hole accretion in brane cosmology. Phys. Rev. Lett. **90**(3), 031 303 (2003). https://doi.org/10.1103/PhysRevLett.90.031303
58. P. Mukherjee, U. Debnath, H. Chaudhary, G. Mustafa, Constraining the parameters of generalized and viscous modified Chaplygin gas and black hole accretion in Einstein-Aether gravity. Eur. Phys. J. C **84**(9), 930 (2024). https://doi.org/10.1140/epjc/s10052-024-13196-5
59. M.U. Shahzad, R. Ali, A. Jawad, S. Rani, Matter accretion onto Einstein–aether black holes via well-known fluids. Chin. Phys. C **44**(6), 065 106 (2020). https://doi.org/10.1088/1674-1137/44/6/065106
60. G. Abbas, A. Ditta, A. Jawad, M. Umair Shahzad, Matter accretion onto a brane-world black hole via Hamiltonian approach. Gen. Relativ. Gravit. **51**(10), 136 (2019). https://doi.org/10.1007/s10714-019-2620-4
61. P. Mukherjee, U. Debnath, A. Pradhan, Accretion phenomena of different kinds of Chaplygin gas models onto Kehagias–Sfetsos black hole in Horava-Lifshitz gravity scenario (2024). https://doi.org/10.48550/arXiv.2410.20367. arXiv:2410.20367
62. G. Abbas, A. Ditta, Matter accretion onto Einstein–power–Maxwell black hole. Gen. Relativ. Gravit. **51**(3), 43 (2019). https://doi.org/10.1007/s10714-019-2527-0
63. G. Abbas, A. Ditta, Matter accretion onto a conformal gravity black hole. Eur. Phys. J. C **80**(12), 1212 (2020). https://doi.org/10.1140/epjc/s10052-020-08787-x
64. P. Mukherjee, U. Debnath, H. Chaudhary, G. Mustafa, How parameter constraining can influence the mass accretion process of a black hole in the generalized Rastall gravity theory? (2024). https://doi.org/10.48550/arXiv.2411.15619. arXiv:2411.15619
65. U. Debnath, Accretion and evaporation of modified Hayward black hole. Eur. Phys. J. C **75**(3), 129 (2015). https://doi.org/10.1140/epjc/s10052-015-3349-1
66. Y. Jia, T.-Y. He, W.-Q. Wang, Z.-W. Han, R.-J. Yang, Accretion of matter by a charged dilaton black hole. Eur. Phys. J. C **84**(5), 1–7 (2024). https://doi.org/10.1140/epjc/s10052-024-12856-w
67. C. Gao, X. Chen, V. Faraoni, Y.-G. Shen, Does the mass of a black hole decrease due to the accretion of phantom energy? Phys. Rev. D Part. Fields Gravit. Cosmol. **78**(2), 024 008 (2008). https://doi.org/10.1103/PhysRevD.78.024008
68. A.J. John, S.G. Ghosh, S.D. Maharaj, Accretion onto a higher dimensional black hole. Phys. Rev. D Part. Fields Gravit. Cosmol. **88**(10), 104 005 (2013). https://doi.org/10.1103/PhysRevD.88.104005
69. A. Ganguly, S.G. Ghosh, S.D. Maharaj, Accretion onto a black hole in a string cloud background. Phys. Rev. D **90**(6), 064 037 (2014). https://doi.org/10.1103/PhysRevD.90.064037

70. D.B. Ananda, S. Bhattacharya, T.K. Das, Acoustic geometry through perturbation of mass accretion rate: radial flow in static spacetimes. Gen. Relativ. Gravit. **47**, 1–20 (2015). https://doi.org/10.1007/s10714-015-1940-2
71. M. Sharif, S. Iftikhar, Shadow of a charged rotating non-commutative black hole. Eur. Phys. J. C **76**, 1–9 (2016). https://doi.org/10.1140/epjc/s10052-016-4472-3
72. M. Sharif, G. Abbas, Phantom accretion by five-dimensional charged black hole. Mod. Phys. Lett. A **26**(23), 1731–1736 (2011). https://doi.org/10.1142/S0217732311036218
73. A.J. John, Black hole accretion in scalar-tensor-vector gravity. Mon. Not. R. Astron. Soc. **490**(3), 3824–3829 (2019). https://doi.org/10.1093/mnras/stz2889
74. A. Ditta, G. Abbas, Relativistic accretion mechanism for some black holes. Chin. J. Phys. **65**, 325–333 (2020). https://doi.org/10.1016/j.cjph.2020.03.007
75. E.P. Gross, Structure of a quantized vortex in boson systems. Il Nuovo Cimento (1955–1965) **20**(3), 454–477 (1961). https://doi.org/10.1007/BF02731494
76. L.P. Pitaevskii, Vortex lines in an imperfect bose gas. Sov. Phys. JETP **13**(2), 451–454 (1961)
77. C. Lan, Y.-G. Miao, Y.-X. Zang, Acoustic regular black hole in fluid and its similarity and diversity to a conformally related black hole. Eur. Phys. J. C **82**(3), 1–20 (2022). https://doi.org/10.1140/epjc/s10052-022-10200-8
78. É. Gourgoulhon, É. Gourgoulhon, Relativistic hydrodynamics, in *Special Relativity in General Frames: From Particles to Astrophysics*, pp. 667–709 (2013). https://doi.org/10.1007/978-3-642-37276-6
79. A.K. Ahmed, M. Azreg-Aıñou, M. Faizal, M. Jamil, Cyclic and heteroclinic flows near general static spherically symmetric black holes. Eur. Phys. J. C **76**, 1–21 (2016). https://doi.org/10.1140/epjc/s10052-016-4112-y
80. F. Ficek, Bondi-type accretion in the Reissner–Nordström-(anti-) de Sitter spacetime. Class. Quantum Gravity **32**(23), 235 008 (2015). https://doi.org/10.1088/0264-9381/32/23/235008
81. P. Mach, E. Malec, Stability of relativistic Bondi accretion in Schwarzschild–(anti–) de Sitter spacetimes. Phys. Rev. D Part. Fields Gravit. Cosmol. **88**(8), 084 055 (2013). https://doi.org/10.1103/PhysRevD.88.084055
82. A.K. Ahmed, M. Azreg-Aıñou, S. Bahamonde, S. Capozziello, M. Jamil, Astrophysical flows near $f(T)$ gravity black holes. Eur. Phys. J. C **76**, 1–13 (2016). https://doi.org/10.1140/epjc/s10052-016-4118-5
83. S. Bahamonde, M. Jamil, Accretion processes for general spherically symmetric compact objects. Eur. Phys. J. C **75**, 1–10 (2015). https://doi.org/10.1140/epjc/s10052-015-3734-9